JMEPEG (2005) 14:671-676
DOI: 10.1361/105994905X64620

1059-9495/$19.00

Deformation Behavior of TC6 Alloy in Isothermal Forging

Xiaoli Li, Miaoquan Li, Dasong Zhu, and Aiming Xiong

(Submitted July 30, 2005)

Isothermal compression of the TC6 alloy was carried out in a Thermecmaster-Z (Wuhan Iron and Steel Corporation, P.R. China) simulator at deformation temperatures of 800~1040 °C, strain rates of 0.001~50.0 s^{-1}, and maximum height reduction of 50%. The deformation behavior of the TC6 alloy in isothermal forging was characterized based on stress-strain behavior and kinetic analysis. The activation energy of deformation obtained in the isothermal forging of the TC6 alloy was 267.49 kJ/mol in the β phase region and 472.76 kJ/mol in the α+β phase region. The processing map was constructed based on the dynamic materials model, and the optimal deformation parameters were obtained. Constitutive equations describing the flow stress as a function of strain rate, strain, and deformation temperature were proposed for the isothermal forging of the TC6 alloy, and a good agreement between the predicted and experimental stress-strain curves was achieved.

Keywords constitutive relationship, high-temperature deformation, processing map, titanium alloy

1. Introduction

The TC6 (Ti-6Al-1.5Cr-2.5Mo-0.5Fe-0.3Si) alloy is a new two-phase alloy that has high relative strength, good resistance against heat and corrosion, good ductility, toughness, and a service temperature of 450 °C, all of which make it an ideal choice for many aerospace applications, for example, aerofoil blade and disc in the aviation and aerospace industries (Ref 1).

To develop processing methods such as forging, it is necessary to characterize the deformation behavior under processing conditions, which include flow stress behavior, deformation mechanisms, and microstructure evolution. Many investigations were carried out on the hot deformation behavior of high-temperature titanium alloys, such as Ti-6Al-4V, IMI834 (Ref 2-7). The hot deformation behavior of Ti-6Al-4V with an equiaxed α-β perform microstructure was modeled in the temperature range of 750~1100 °C and strain rate range 0.0003~100 s^{-1} by Seshacharyulu et al. (Ref 2). Wanjara et al. (Ref 4) investigated the flow stress behavior of near-α alloy IMI834 by compression testing at isothermal deformation conditions of different deformation temperature and strain rates up to a strain of 0.8.

The two-phase TC6 alloy was developed recently, and not much information about deformation behavior is available. In this paper, isothermal compression was conducted at different temperatures, strain rates, and height reduction during the high-temperature deformation of the TC6 alloy, and the deformation behavior was investigated.

2. Experimental Procedures

The TC6 titanium alloy produced by Baoji nonferrous metal works, P.R. China, is 42 mm in diameter. Its chemical composition is shown in Table 1. The heat treatment procedure before isothermal compression was to heat at 870 °C, keep for 1 h, adjust to 650 °C, keep for 2 h, and cool in air to room temperature. Cylinder specimens 8 mm in diameter and 12 mm in height were machined from the heat-treated bars, and the cylinder ends were grooved for retention of the glass lubricants used during isothermal compression tests.

To investigate the effects of process parameters on deformation behavior of the TC6 alloy in isothermal compression, the nominal deformation temperatures were arranged as 800-1040 °C at intervals of 30 °C and the strain rates as 0.001-50.0 s^{-1} for each deformation temperature. Isothermal compression was performed to 50% of maximum height reduction at each combination of deformation temperatures and strain rates. The isothermal compression experiments with constant strain rate were conducted on a Thermecmaster-Z simulator for hot working with optical dilatometer (Wuhan Iron and Steel Corporation, P.R. China). The specimens were kept for 3 min at the deformation temperature before the commencement of deformation to ensure well-proportioned temperature fields. After compression, the specimens were immediately quenched by nitrogen gas at the cooling speed of 30 °C/s to retain the as-deformed microstructures.

The load-stroke data were converted to stress-strain curves using standard equations. The flow stress was obtained as a function of deformation temperature, strain rate, and strain. The activation energy of deformation and processing map were generated from the experimental data.

3. Results and Discussion

3.1 Flow Stress

Typical stress-strain curves in the (α+β) region and β region of TC6 titanium alloys are shown in Fig. 1. These curves

Table 1 Chemical composition of a TC6 titanium alloy, wt.%

Al	Cr	Fe	Mo	Si	Ti
6.29	1.42	0.42	2.71	0.33	bal.

Xiaoli Li, Miaoquan Li, Dasong Zhu, and **Aiming Xiong,** School of Materials Science and Engineering, Northwestern Polytechnical University, Xi'an 710072, P.R. China. Contact e-mail: nwpulily@yahoo.com.cn.

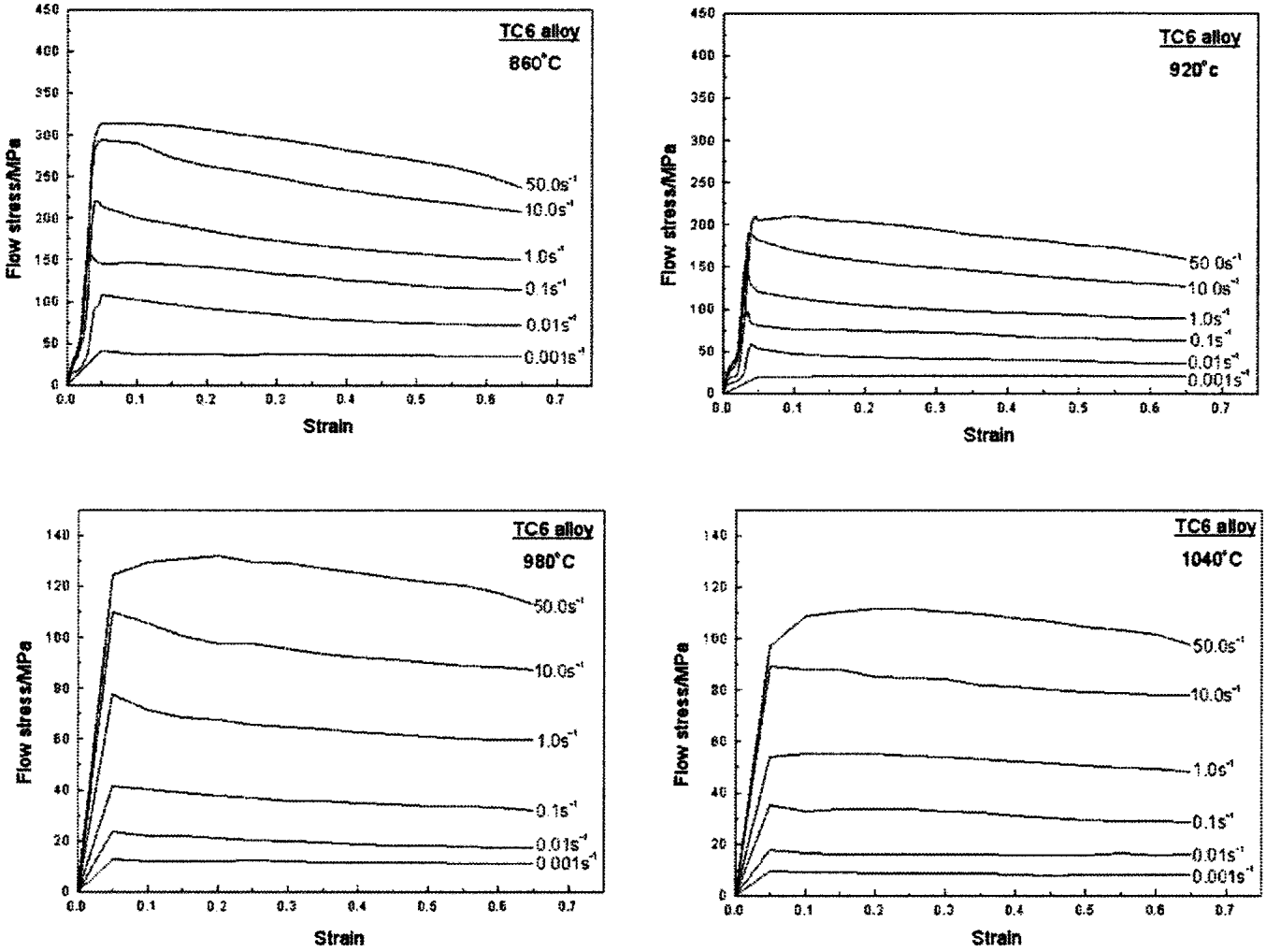

Fig. 1 True stress-strain curves of the TC6 titanium alloys during isothermal compression

show that the flow stress decreases with an increasing deformation temperature for the given strain rate, and the flow stress increases with the increasing of strain rate for the given temperature. As can be seen in Fig. 1, the curves exhibit a flow-softening behavior in which the flow stress reaches a peak at a critical strain and then decreases with further straining. The critical strain from the peak stress to the steady flow increases with increasing strain rates. The peak stress in the isothermal compression of the TC6 alloy is shown in Fig. 2(b). From Fig. 2(b), the effect of deformation temperature on peak stress is shown to be slight at a lower strain rate, otherwise there is a significant effect. The peak stress of the alloy has a slope drop and then is steady above a deformation temperature of 960 °C, which results from dynamic recrystallization. The steady flow stress in the isothermal deformation of the TC6 alloy is shown in Fig. 2(a). From Fig. 2(a), the steady flow stress in the isothermal compression of the TC6 alloy is shown to be sensitive to the strain rate but not to a deformation temperature above 960 °C.

Most plastic power converts to heat and results in a temperature rise in the high temperature deformation process. If the strain increment is $\Delta\varepsilon$ and the homogeneous temperature rise ΔT can be calculated in the in Eq 1 (Ref 8):

$$\Delta T = \frac{\eta}{\rho c}\int_0^{\bar{\varepsilon}} \bar{\sigma} d\bar{\varepsilon} \qquad \text{(Eq 1)}$$

where c is the specific heat (J/g·K^{-1}), ρ is the material density (g/cm^3), $\bar{\sigma}$ and $\bar{\varepsilon}$ is the equivalent stress (MPa) and strain, η is thermal efficiency being calculated by Eq 2.

$$\eta = \begin{cases} 1 & \dot{\varepsilon} \geq 1.0\ \mathrm{s}^{-1} \\ \frac{1}{3}(3 + 1\mathrm{g}\dot{\varepsilon}) & 0.001\ \mathrm{s}^{-1} < \dot{\varepsilon} < 1.0\ \mathrm{s}^{-1} \\ 0 & \dot{\varepsilon} \leq 0.001\ \mathrm{s}^{-1} \end{cases} \qquad \text{(Eq 2)}$$

According to Eq 1 and 2, the temperature rise in the isothermal compression of the TC6 alloy was calculated and is illustrated in Table 2. The actual deformation temperature in the high-temperature deformation of the TC6 alloy will increase with the temperature elevation resulting from plastic deformation.

3.2 Kinetic Analysis

The dependence of flow stress on the deformation temperature and strain rate at high-temperature deformation is generally expressed in terms of a kinetic equation given by:

$$\dot{\varepsilon} = \mathrm{A}\sigma^n \exp(Q/\mathrm{R}T) \qquad \text{(Eq 3)}$$

where A is a constant, $\dot{\varepsilon}$ is the strain rate (s^{-1}), σ is the flow stress (MPa), Q is the activation energy of deformation (kJ/

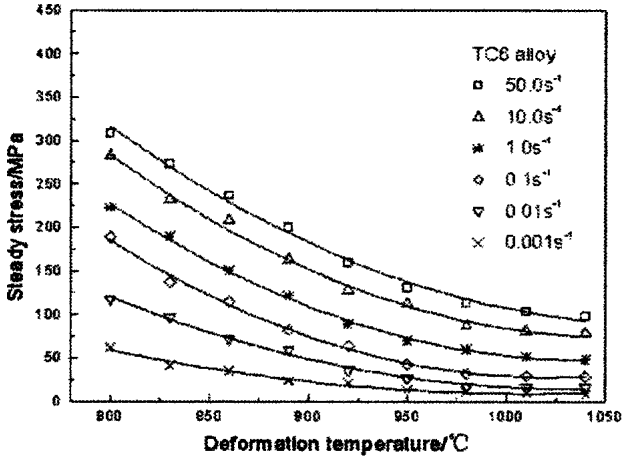

(a) Steady stress

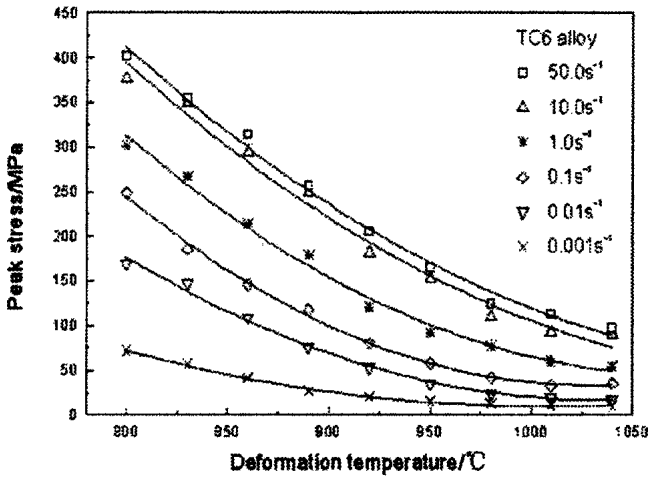

(b) Peak stress

Fig. 2 Steady and peak stress during isothermal compression of the TC6 alloy

Table 2 Calculated temperature rise during isothermal compression of the TC6 alloy

Deformation temperature, °C	Strain rates, s^{-1}				
	50	10.0	1.0	0.1	0.01
800	29.88	26.82	21.11	12.32	3.67
830	26.44	23.29	18.09	8.93	3.08
860	22.98	19.67	13.84	6.98	2.25
890	18.80	15.93	11.26	5.13	1.78
920	15.14	11.82	7.98	3.76	1.10
950	12.30	10.30	6.10	2.62	0.78
980	10.08	7.62	5.19	1.92	0.53
1010	9.12	6.82	4.45	1.75	0.46
1040	8.60	6.65	4.23	1.69	0.43

mol), R is the gas constant (8.314 J/mol·K^{-1}), T is the absolute deformation temperature (K), and n is the stress exponent.

To identify the high-temperature deformation mechanism,

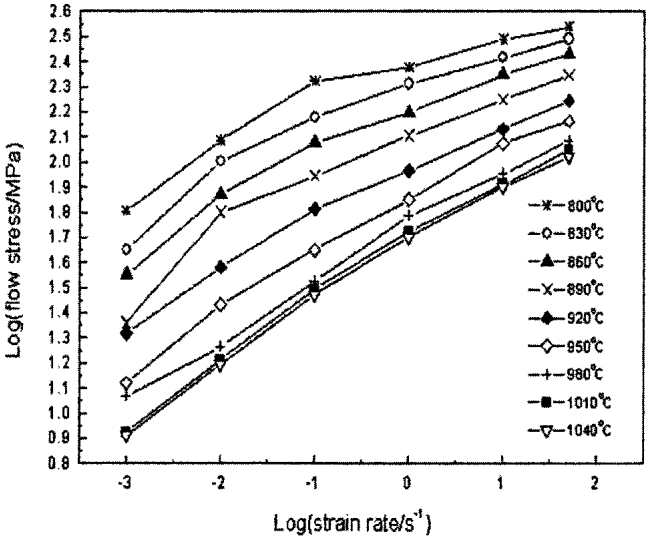

Fig. 3 Variation of the flow stress with deformation temperature and strain rate

the kinetic parameters n and Q in Eq 3 are to be evaluated. From Fig. 3, it is seen that n is strain rate and temperature dependent when considered over the entire range of strain rate and temperature used in this study. The activation energy of deformation will represent the workability of materials and could be calculated by the Eq 4 (Ref 9).

$$Q = -R \left.\frac{\partial \ln \dot{\varepsilon}}{\partial \frac{1}{T}}\right|_{\sigma} \approx -R \left.\frac{\Delta \ln \dot{\varepsilon}}{\Delta \frac{1}{T}}\right|_{\sigma} \quad \text{(Eq 4)}$$

The $(\alpha+\beta) \rightarrow \beta$ transus for this studied TC6 titanium alloys is about 960 °C, and so the kinetic parameters may be evaluated separately in the two-phase region (800~950 °C) and the single-phase region (980~1040 °C). The flow stress values are markedly different in these two regions.

In the $(\alpha+\beta)$ region, the value of stress exponent, n, is estimated to be about 5.06. The apparent activation energy is estimated as about 472.76 kJ/mol. In the β region, the value of the stress exponent, n, is estimated to be about 4.46. The apparent activation energy estimated is about 267.49 kJ/mol.

3.3 Processing Map

The TC6 alloy is one of the difficult deformed alloys, which has poor formability resulting in limited deformation temperature ranges and great variation of flow stress with deformation temperature and/or strain rate. The characterization of deformation behavior is thus essential for the optimization of hot forging processes. The deformation behavior at high temperature has been modeled using the approach of processing maps, which are generated on the basis of the principles of the dynamic materials model (DMM) (Ref 10, 11). The DMM approach assumes that the instantaneous power P absorbed by the workpiece during plastic flow is dissipated by the dissipator content G, which is the power dissipated by plastic work and the dissipator co-content J, which is the work related to the metallurgical mechanisms that occur dynamically to dissipate power. Plastic instability and fracture processes are associated

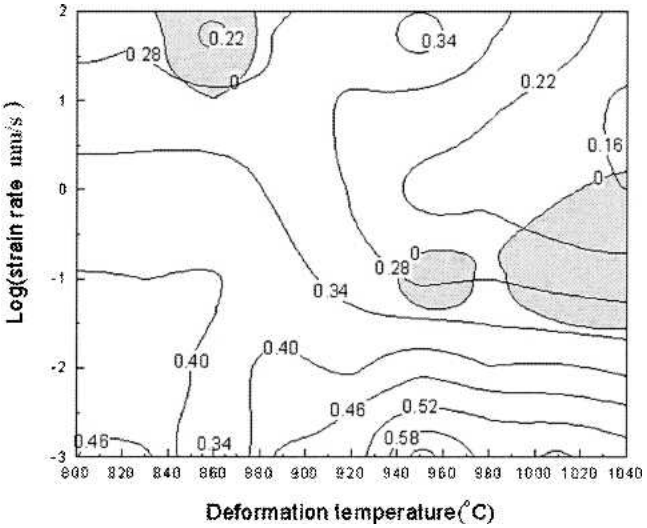

Fig. 4 Processing map of the TC6 alloy at a strain of 0.5

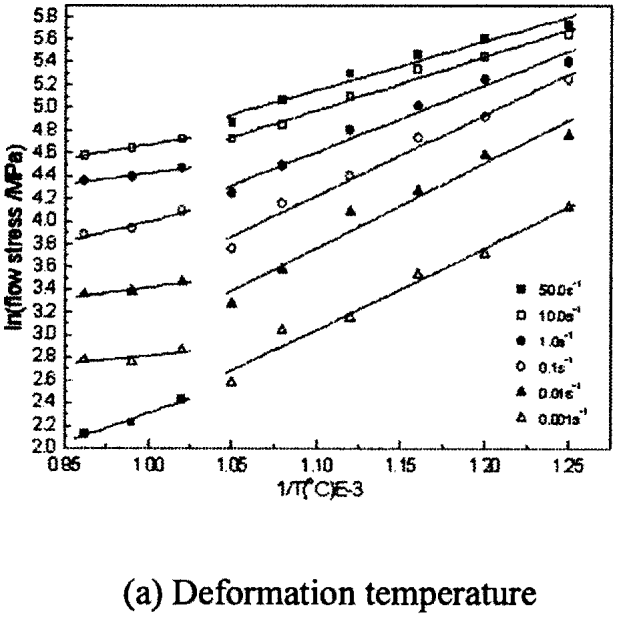

Fig. 5 Variation of the flow stress with deformation temperature and strain

with G, and microstructure evolution is associated with J. The power P absorbed by the workpiece during plastic flow can be written as:

$$P = \bar{\sigma}\,\dot{\bar{\varepsilon}} = \int_0^{\bar{\sigma}} \dot{\bar{\varepsilon}}\, d\bar{\sigma} + \int_0^{\dot{\bar{\varepsilon}}} \bar{\sigma}\, d\dot{\bar{\varepsilon}} = J + G \qquad \text{(Eq 5)}$$

where $\bar{\sigma}$ is the equivalent stress and $\dot{\bar{\varepsilon}}$ the equivalent strain rate.

The partitioning of power between J and G is given by Eq 6.

$$\frac{dJ}{dG} = \frac{\dot{\bar{\varepsilon}}\, d\bar{\sigma}}{\bar{\sigma}\, d\dot{\bar{\varepsilon}}} = \frac{d(\log \bar{\sigma})}{d(\log \dot{\bar{\varepsilon}})} \qquad \text{(Eq 6)}$$

The ratio is equivalent to the strain rate sensitivity parameter, m. The strain rate sensitivity m is a power partitioning index that disperses the energy for plastic deformation (G) and the energy for the metallurgical mechanism (J).

The dissipator co-content J can be described as:

$$J = \frac{m}{m+1}\,\sigma\dot{\varepsilon} \qquad \text{(Eq 7)}$$

The efficiency of power dissipation η can be defined as:

$$\eta = \frac{J}{J_{\max}} = \frac{2m}{m+1} \qquad \text{(Eq 8)}$$

The parameter η is a dimensionless parameter, indicating how efficiently the material dissipates energy by microstructure changes and to determine the optimum conditions for thermomechanical processing. The variation of η with temperature and strain rate gives the power dissipation map, which characterizes microstructural changes occurring during hot deformation. In the theory proposed by Kumar (Ref 12), the regimen where the metallurgical instability occurs during plastic flow was obtained when the following instability condition is satisfied,

$$\xi(\dot{\varepsilon}) = \frac{\partial \log \frac{m}{m+1}}{\partial \log \dot{\varepsilon}} + m < 0 \qquad \text{(Eq 9)}$$

where $\xi(\dot{\varepsilon})$ is called the instability parameter, the variation of which with temperature and strain rate constitutes an instability map. The instability map may be superimposed on the power dissipation map to obtain a processing map that not only exhibits the domains characteristic of different mechanisms but also the regimes in which microstructural instabilities occur.

The processing map obtained at 0.5 strains is presented in Fig. 4. The contour numbers indicate the efficiency of power dissipation η, and the shaded areas represent unstable regions. The region in which the value of this parameter $\xi(\dot{\varepsilon})$ becomes

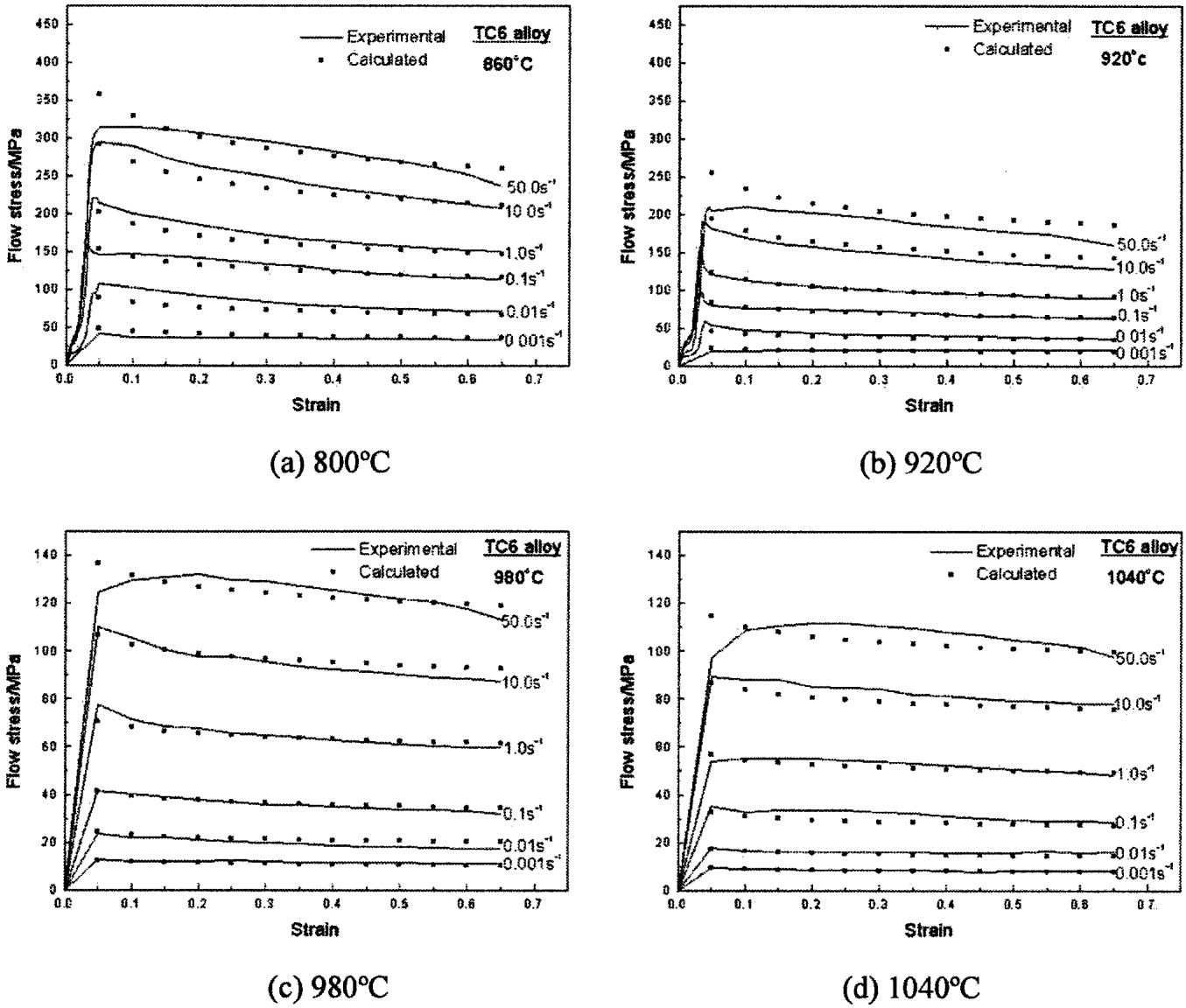

Fig. 6 Comparison of the calculated with the experimental flow stress

Table 3 Material constants in Eq 14

	Strain rates $\dot{\varepsilon}$	B_0	B_1	B_2	B_3	B_4
($\alpha + \beta$)	$<1.0\ s^{-1}$	14.7491	−1.4469	0.0426	−0.0004	−0.1089
region	$\geq 1.0\ s^{-1}$	−15.2824	0.4741	0.0017	−0.0001	−0.1244
β region	$<1.0\ s^{-1}$	31.3844	−4.8599	0.2559	−0.0042	−0.0738
	$\geq 1.0\ s^{-1}$	6.9398	−0.7682	0.0397	0.0006	−0.0548

negative characterizes the possibility of unstable flow. The greater the negative magnitude of the parameter, the greater the chances of unstable flow. The map shows a peak efficiency of 0.67 at about 950 °C and 10^{-3} s^{-1}, indicating that the region is an optimum condition for thermomechanical processing of this alloy. The unstable regions are observed in three areas. The first domain of unstable region occurs at 830~880 °C and 10.0~100.0 s^{-1}, the second at 940~970 °C and 0.040~0.251 s^{-1}, and the last at 980~1040 °C and 0.025~1.585 s^{-1}. The hot forming should not be performed in the three unstable regions to avoid the occurrence of the fracture.

3.4 Constitutive Equation for Plastic Deformation

The flow stress of an alloy depends on a number of test variables, including chemical composition, strain rate, strain, and deformation temperature. Figure 3 shows the variation of flow stress with strain rate at different temperatures, Fig. 5(a) is the variation of flow stress with deformation temperature at different strain rates, and Fig. 5(b) is the variation of flow stress with strain at different deformation temperature. The steady-state rate equation in the high-temperature deformation relates the flow stress with the deformation temperature, strain rate, and strain as:

$$\varepsilon^m \dot{\varepsilon} \exp\left(\frac{Q}{RT}\right) = A\sigma^n \qquad \text{(Eq 10)}$$

where A is a constant, $\dot{\varepsilon}$ is the strain rate (s^{-1}), σ is the flow stress (MPa), ε is the strain, Q is the activation energy of deformation (kJ/mol), R is the gas constant (kJ/mol·K^{-1}), T is the absolute deformation temperature (K), n is the stress exponent, and m is the strain exponent.

By taking logarithm, Eq 10 can be written as:

$$\ln \sigma = \frac{\ln A}{n} + \frac{1}{n}\left(\ln \dot{\varepsilon} + \frac{Q}{RT}\right) + \frac{m}{n}\ln \varepsilon \quad \text{(Eq 11)}$$

where A, B, and C are material constants.

The temperature-compensated strain rate parameter or the Zener-Hollomon parameter Z is defined as:

$$Z = \dot{\varepsilon} \exp\left(\frac{Q}{RT}\right) \quad \text{(Eq 12)}$$

Introducing the Zener-Hollomon parameter into Eq 11, Eq 11 can be modified as:

$$\ln \sigma = A + B \ln Z + C \ln \varepsilon \quad \text{(Eq 13)}$$

where A, B, and C are material constants.

To describe accurately the deformation behavior of the TC6 alloy in isothermal forging, Eq 13 is improved as:

$$\ln \sigma = B_0 + B_1 \ln Z + B_2 (\ln Z)^2 + B_3 (\ln Z)^3 + B_4 \ln \varepsilon \quad \text{(Eq 14)}$$

where B_0, B_1, B_2, B_3, and B_4 are material constants.

The TC6 alloy is very sensitive to strain rate, so the material constants in the constitutive Eq 14 should be different in various strain rate region. By regression analysis to Eq 14 in various strain regions separately, the material constants are determined and are shown in Table 3.

Substituting the material constants in Table 3 into Eq 14, flow stress can be computed at different deformation conditions. Figure 6 illustrates a comparison of the calculated flow stress of the TC6 alloy with the experimental. The mean difference between the calculated with the experimental flow stress is 6.73%.

4. Conclusions

During the isothermal deformation of a TC6 alloy, the deformation behavior is affected significantly by the process parameters, including the deformation temperature, height reduction, and strain rate.

- The deformation temperature and strain rate affect the peak and steady stress in the isothermal deformation of the TC6 alloy greatly. The peak and steady stress decrease with an increase of deformation temperature and a decrease of strain rate.
- The activation energy of deformation in the high-temperature deformation of TC6 alloy was estimated to be 267.49 kJ/mol in the β phase region and 472.76 kJ/mol in the (α+β) phase region.
- By construction of the processing map of the TC6 alloy, three unstable deformation regions were obtained, in which the first unstable region occurs at 830~880 °C and 10.0~100.0 s^{-1}, the second at 940~970 °C and 0.040~0.251 s^{-1}, and the last at 980~1040 °C and 0.025~1.585 s^{-1}. The combination of the deformation temperature with strain rate should be avoided in the high-temperature deformation of the TC6 alloy.
- The constitutive equations describing flow stress as a function of strain rate, strain, and deformation temperature were established by employing the Arrhenius equation, and a good agreement between the calculated results and the experimental data was achieved.

Acknowledgments

This work was financially supported by Natural Science Foundation Grant 50475144, State Key Foundational Research Plan Grant G2000067206, a Teaching and Research Award Fund for Outstanding Young Teachers in Higher Education Institutions of MOE, and the Doctorate Creation Foundation of Northwestern Polytechnical University Grant CX200305, P.R. China.

References

1. M. Li, S. Chen, A. Xiong, H. Wang, S. Su, and L. Sun, Acquiring a Novel Constitutive Equation of a TC6 Alloy at High-Temperature Deformation, *J. Mater. Eng. Perform.,* Vol 14, 2005, p 163-266
2. T. Seshacharyulu, S.C. Medeiros, W.G. Frazier, and Y.V.R.K. Prasad, Hot Working of Commercial Ti-6Al-4V with an Equiaxed α-β Microstructure: Materials Modeling Considerations, *Mater. Sci. Eng. A,* Vol 284, 2004, p 184-194
3. N.-K. Park, J.-T. Yeom, and Y.-S. Na, Characterization of Deformation Stability in Hot Forging of Conventional Ti-6Al-4V Using Processing Maps, *J. Mater. Proc. Technol.,* Vol 130-131, 2002, p 540-545
4. P. Wanjara, M. Jahazi, H. Monajati, S. Yue, and J.P. Immarigeon, Hot Working Behavior of Near-α Alloy IMI834, *Mater. Sci. Eng. A,* Vol 396, 2005, p 50-60
5. Y. Liu and T.N. Baker, Deformation Characteristic of IMI685 Titanium Alloy under β Isothermal Forging Conditions, *Mater. Eng. A,* Vol 197, 1995, p 125-131
6. L.X. Li, Y. Lou, L.B. Yang, D.S. Peng, and K.P. Rao, Flow Stress Behavior and Deformation Characteristics of Ti-3Al-5V-5Mo Compressed at Elevated Temperatures, *Mater. Design,* Vol 23, 2002, p 451-457
7. D. Weinem, J. Kumpfert, M. Peters, and W.A. Kaysser, Processing Window of the Near-α-Titanium Alloy TIMETAL-1100 to Produce a Fine-Grained β Structure, *Mater. Sci. Eng. A,* Vol 206, 1996, p 55-62
8. S. Tingchun and C. Sencan, Experimental Study on TC4 Titanium Alloy High-Temperature Constitutive Equation, *Forging Stamping Technol.,* Vol 3, 1999, p 22-24 (in Chinese)
9. W. Roberts, Deformation, *Processing and Structure,* American Society for Metals, Metal Park, OH, 1984, p 109-184
10. H.J. Front and M.E. Ashby, *Deformation Maps,* Pergamon Press, New York, 1982
11. Y.V.R.K. Prasad and H.L. Gegel, Modeling of Dynamic Material Behavior in Hot Deformation: Forging of Ti-6242, *Metall. Trans. A,* Vol 15, 1984, p 1883-1892
12. A.K.S. K. Kumar, "Criteria for Predicting Metallurgical Instabilities in Processing," M.Sc. (Eng) thesis, Indian Institute of Science, Bangalore, India, 1987